Journal of Physics Communications

PAPER

Hydrogen detection using membrane-type surface stress sensor

Taro Yakabe[1], Gaku Imamura[2], Genki Yoshikawa[3], Masahiro Kitajima[1] and Akiko N Itakura[1]

[1] Research Center for Advanced Measurement and Characterization, National Institute for Materials Science (NIMS), 1-2-1 Sengen, Tsukuba, Ibaraki, 305-0047, Japan
[2] International Center for Materials Nanoarchitectonics, National Institute for Materials Science (NIMS), 1-1 Namiki, Tsukuba, Ibaraki, 305-0044 Japan
[3] Center for Functional Sensor & Actuator, National Institute for Materials Science (NIMS), 1-1 Namiki, Tsukuba, Ibaraki, 305-0044 Japan

E-mail: yakabe.taro@nims.go.jp

Keywords: hydrogen, MSS, langmuir, adsorption, absorption

OPEN ACCESS

RECEIVED
12 November 2019

REVISED
3 February 2020

ACCEPTED FOR PUBLICATION
5 February 2020

PUBLISHED
13 February 2020

Abstract

This study shows a possibility of the application of a membrane-type surface stress sensor (MSS) with a Pd film to a hydrogen sensor. It was able to detect hydrogen concentrations from 5 to 40000 ppm in a nitrogen gas mixture. In the case of a conventional sensor using a hydrogen-occluding material, it is necessary to wait for a state of saturation. In contrast, the proposed method can detect hydrogen quickly by the initial rate of hydrogen absorption. The relationship between the initial absorption rate and hydrogen concentration is explained by considering the two-step reaction kinetics of hydrogen absorption into bulk Pd via Langmuir dissociative adsorption on surface.

1. Introduction

Hydrogen is known as a clean and renewable energy carrier. The demand for hydrogen is expected to increase worldwide every year. Hydrogen is produced by reforming natural gas, or the electrolysis of water, biomass, a byproduct of steelworks, and so on. It is supplied to fuel cells, hydrogen automobiles, and power generations. The transport and storage of hydrogen must be performed in a safe manner. Therefore, it is also indispensable to develop hydrogen sensors that detect hydrogen leaks. Various techniques of hydrogen detection have been developed so far; these include catalytic, thermal conduction, electrochemical, resistance-based, work-function based, mechanical, optical, and acoustic techniques [1]. Here are some details on the mechanical method associated with our study. Hydrogen absorption would lead to stress formation of some materials. The stress measurements of them are applied to hydrogen sensing. The advantage of sensors by the stress measuring is that they can be applied to various gas sensors with selecting sensitive films. Attempts to use micro-cantilevers, which were known as atomic force microscope probes [2], as stress sensors began in the 90's [3], and the first trial for detecting hydrogen by using a cantilever sensor was executed with its adsorption on a Pt film [4]. The cantilever sensor was improved by using hydrogen-storage materials [5, 6]. Hydrogen penetrates into the bulk after dissociation at the surface [7]. For example, Pd expands by absorbing hydrogen; this hydrogen-absorbed Pd has low- and high-hydrogen-concentration phases (α and α', respectively). The lattice constants of Pd, Pd-H (α), and Pd-H(α') are 0.38874 nm, 0.3895 nm, and 0.4025 nm, respectively [7]. A membrane-type surface stress sensor (MSS) was developed by optimizing a standard piezoresistive cantilever [8]. It has two-order higher sensitivity than a standard piezoresistive cantilever [9]. As shown in figure 1(a), the outline of the MSS design is as follows. The stress of the sensitive film on the disk is transmitted to the four narrow piezoresistive parts that support the disk and constitute a Wheatstone bridge circuit. Thus, the sensor can observe signals according to the stress with high sensitivity. Studies have used the finite element analysis to study the mechanism of MSS for various gas detections through experiments, theoretical models, and numerical simulations [10–12].

In this paper, we report on hydrogen-concentration measurements by using MSS with a Pd thin film. Furthermore, in this study, by focusing on the initial process of hydrogen absorption, we solved the conventional problem of the utilization of a large amount of time for measuring the saturation state. In addition, the relationship between hydrogen concentration and initial reaction rate is explained simply by the two-step reaction kinetics of hydrogen absorption into bulk Pd via Langmuir dissociative adsorption on the surface.

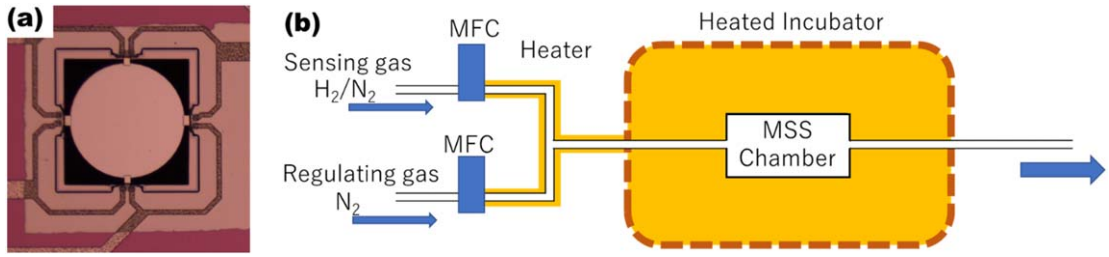

Figure 1. (a) Optical microscope image of MSS with a Pd film. The diameter of the disk is 300 μm. (b) Schematic of our experimental system. Hydrogen concentration with nitrogen is adjusted by two mass-flow controllers (MFCs).

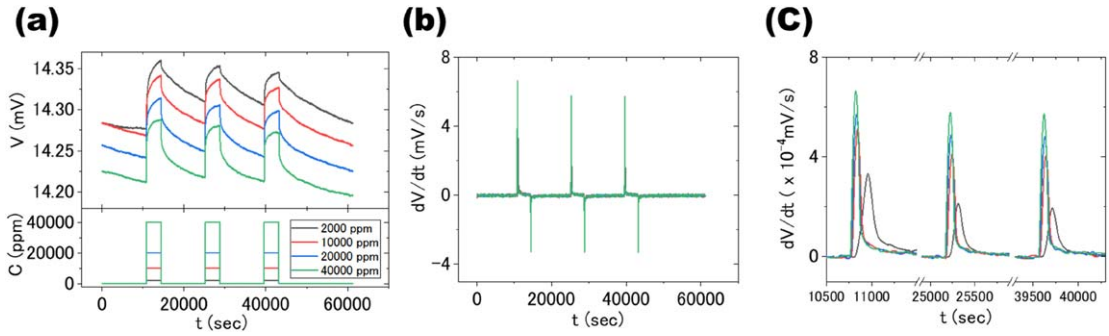

Figure 2. MSS signals for hydrogen concentrations of 2000 ppm (black), 10000 ppm (red), 20000 ppm (blue), and 40000 ppm (green). (a) Observed voltage signals of MSS (V) and concentration of hydrogen (C) with time (t). (b) Numerical differentiation (dV/dt) of the voltage signal curves in (a). (c) Enlargement around the upward convex peaks in (b).

2. Experimental methods

Figure 1(a) shows MSS with a Pd film. The film was deposited by an electron beam bombardment, the target was a 99.9% Pd nugget, and the deposition rate was approximately 0.1 nm s^{-1}. The film thickness was 20 nm, which was measured using a quartz crystal thickness monitor during evaporation. Figure 1(b) shows our experimental set up, in which two kinds of sensing-gas sources of hydrogen and nitrogen were used in cylinders, the hydrogen concentrations of which were 40000 ppm (4.00%) $\pm$ 100 (0.01%) ppm and 100 ppm $\pm$ 10 ppm, respectively. Each of the sensing gas lines was further diluted with pure nitrogen (99.999%) from the other regulating gas line. The hydrogen concentration in the MSS chamber was controlled by two mass-flow controllers (MFC, SEC-N112MGM of Horiba STEC). The amount of the flowing gas was 30 sccm. We varied the concentration of hydrogen from 2000 ppm to 40000 ppm by using the 40000-ppm hydrogen in one cylinder and from 5 ppm to 100 ppm by using the 100-ppm hydrogen in the other cylinder. The MSS with a Pd film was mounted in the MSS chamber sealed with O-rings. The MSS chamber and gas line were placed in a heated incubator with ribbon heaters (orange-colored region in figure 1(b)). The temperature was controlled at 333.15 K $\pm$ 0.02 K. For each concentration of hydrogen, one experimental procedure consisted of three cycles of 1-h hydrogen injection and 3-h pure nitrogen purge, with the stress being measured using the MSS. The Pd film immediately after deposition showed large stress and low reproducible signals during hydrogen exposure. The low reproducibility was due to the hysteresis of hydrogen absorption and desorption [13]. Before measuring the hydrogen concentration, we performed absorption and desorption more than 10 times by using the 40000-ppm hydrogen gas to suppress hysteresis. The stress signals were read as electrical voltages of MSS in the sampling time of 1 s (*i.e.*, 1-Hz measurement).

3. Results and discussions

Figure 2 shows the MSS signals for hydrogen concentration from 2000 to 40000 ppm. In figure 2(a), the horizontal axis represents time t, and the vertical axes represent the signals of MSS (V) and the concentration of hydrogen (C) under the MFC regulation. These curves show the hydrogen concentrations of 2000 ppm (black), 10000 ppm (red), 20000 ppm (blue), and 40000 ppm (green). The signals showed noticeable increase just after 10800 s, 25200 s, and 39600 s, which corresponded to regulated hydrogen injection times. The signals decreased

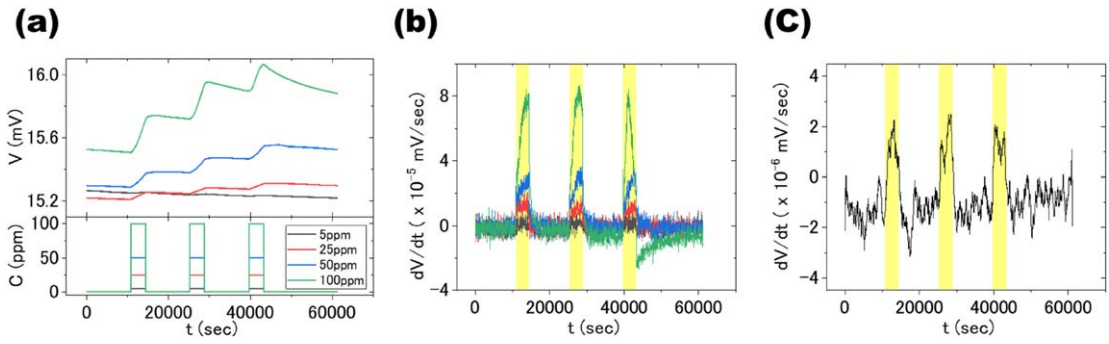

Figure 3. MSS signals for hydrogen concentrations of 5 ppm (black), 25 ppm (red), 50 ppm (blue), 100 ppm (green). (a) Observed voltage signals of MSS (V) and hydrogen concentration (C) with time (t). (b) Numerical differentiation (dV/dt) in (a). (c) Numerical differentiation of 5-ppm curves in (a). More adjacent points were adopted.

just after 14400 s, 28800 s, and 43200 s, which are the nitrogen purging times. In the observation of the changes in the signals of the hydrogen injections for 1 h, the signal for 40000 ppm seemed to approach saturation but the other signals for 20000 ppm, 10000 ppm, and 2000 ppm needed more time to saturate. It was difficult to use these signals directly for determining the concentration because saturation took $\geqslant$1 h and gradual changes were observed in the baseline. Therefore, we focused on the sharp changes over time and made numerical differentiations, as shown in figure 2(b), by using a standard data analysis and graphing software. The numerical smoothing was performed using a second-order polynomial and 101 adjacent points, corresponding to $\pm$ 50 s. The change of the MSS signal is proportional to the stress of the sensitive film [8, 9]. which in turn is proportional to the amount of absorbed hydrogen [5, 6]. Therefore, the time differentiation of the MSS signal corresponds to the hydrogen-absorption rate. The upward and downward convex peaks are clearly observed immediately after the hydrogen injection and nitrogen purge, respectively. Figure 2(c) shows enlargements around the upward convex peaks in fugure 2(b); these enlargements correspond to the changes in the hydrogen absorption rate in the initial process. The peak in the green curve (40000-ppm hydrogen) is the largest, while those in the blue (20000 ppm), red (10000 ppm), and black (2000 ppm) curves decreased. The peak heights immediately after the first injection of hydrogen were approximately 20% higher than those after the second and third injections. We consider that this difference is caused by the remaining hysteresis of hydrogen absorption and desorption in Pd.

Furthermore, we confirmed that the MSS detected signals at lower hydrogen concentrations. Figure 3 show the signals of MSS for hydrogen concentration from 5 ppm to 100 ppm. In figure 3(a), the horizontal and vertical axes are the same as those in figure 2(a). These curves show the hydrogen concentrations of 5 ppm (black), 25 ppm (red), 50 ppm (blue), and 100 ppm (green). The signals do not show sudden increase and decrease as those in figure 2(a), but slowly increased with hydrogen injections. Figure 3(b) shows numerical differentiation by using the same method and the same number of adjacent points as that used in figure 2(b). The peaks at 100 ppm, 50 ppm, and 25 ppm are clearly defined and their heights are reproducible. The peak at 5-ppm hydrogen injection is not clear and appears buried in noise. When we adopted 1001 adjacent points, remarkable peaks were defined, as shown in figure 3(c). These show a trade-off between the detectable region size of the hydrogen concentrations and the brevity of the necessary time required for the concentration measurement. From a practical point of view, suitable number of adjacent points should be selected.

Figure 4 shows the relation between hydrogen concentrations and the peak heights of differentiations in figures 2(c) and 3(b). The peak height at each concentration from 25 to 40000 ppm upon hydrogen injection is plotted. The peak heights immediately after the first, second, and third hydrogen injections are represented by black squares, red circles, and blue triangles, respectively, in figures 2(c) and 3(b). These points are fitted by the equation (6), and this physical mechanism is explained as follows. Assuming a two-step reaction process in figure 5, hydrogen molecules are dissociated into atoms on the Pd surface and each atom is absorbed into the bulk [14–16]. The process is represented by the following chemical reaction formula:

$$\mathrm{Pd(s)} + \frac{1}{2}\mathrm{H_2} \underset{k_{1-}}{\overset{k_{1+}}{\rightleftarrows}} \mathrm{Pd(s)} - H \underset{k_{2-}}{\overset{k_{2+}}{\rightleftarrows}} \mathrm{PdH}, \tag{1}$$

where Pd(s)-H, PdH, and $k_i (I = 1+, 1-, 2+, 2-)$ imply the status of H-atom adsorption on the Pd surface, the status of H-atom storage in Pd bulk, and the reaction-rate constants, respectively (figure 5). We assume that (i) reaction 1 is much faster than reaction 2 (*i.e.*, reaction 2 is the rate-determining step), (ii) Pd(s)-H is Langmuir dissociated adsorption, and (iii) the concentration of PdH is zero (*i.e.*, [PdH] $\sim$ 0) in the initial state. From assumptions (i) and (ii),

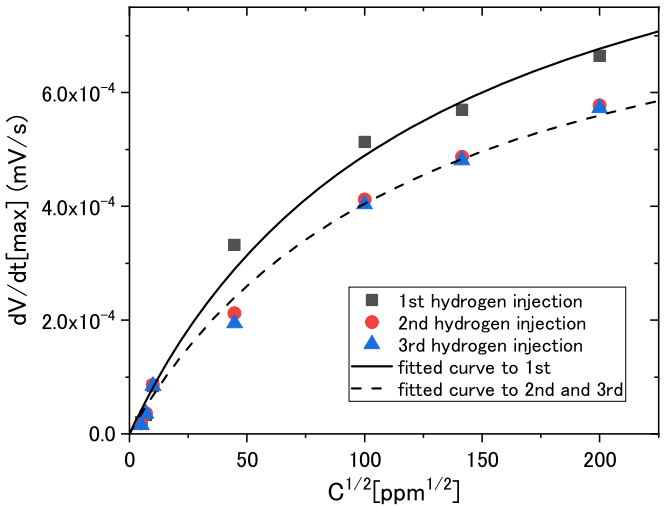

Figure 4. Square root of hydrogen concentration ($C^{1/2}$) versus local maximum peak height of differential (dV/dt [max]). The maximum value of the derivative at each concentration from 25 ppm to 40000 ppm upon hydrogen injection is plotted. The peak heights after the first (black square), second (red circle), and third (blue triangle) hydrogen injections in figures 2(c) and 3(b). These points are fitted by the Langmuir dissociative adsorption model.

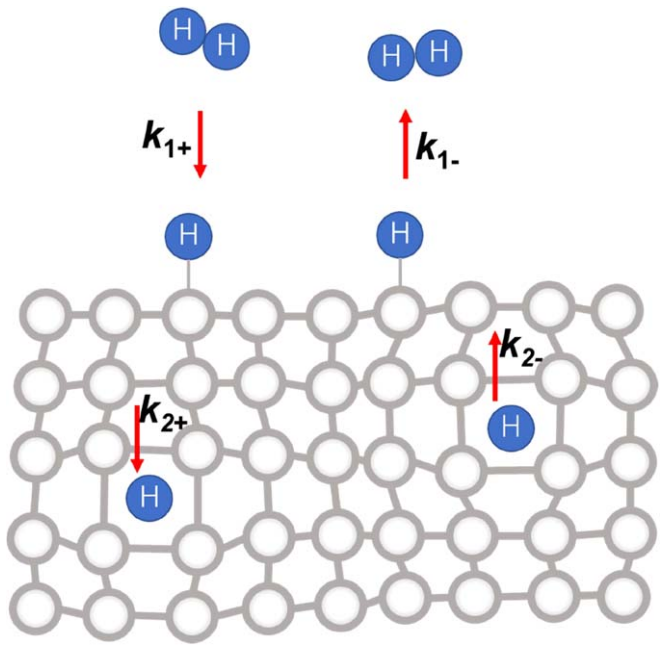

Figure 5. Model schematic: hydrogen molecules are adsorbed on the surface and dissociated atoms are absorbed into the Pd film. The adsorbed hydrogens expand the lattice and the stress is caused. The blue and white atoms represent H and Pd, respectively.

$$[\mathrm{Pd(s)} - \mathrm{H}] \propto \frac{K\sqrt{C}}{1 + K\sqrt{C}}, \tag{2}$$

where C is the concentration of hydrogen in the mixture gas with nitrogen and is proportional to the partial pressure of hydrogen, and $K = k_{1+}/k_{1-}$ [17]. Based on the rate equation of reaction 2 and assumption (iii),

$$\frac{d[\mathrm{PdH}]}{dt} = k_{2+}[\mathrm{Pd(s)} - \mathrm{H}] - k_{2-}[\mathrm{PdH}]$$
$$\tilde{} \; k_{2+}[\mathrm{Pd(s)} - \mathrm{H}]. \tag{3}$$

As PdH is used to input stress to the MSS and the change in the MSS signal (V) is proportional to the stress [11],

$$V - V_0 \propto [\mathrm{PdH}], \tag{4}$$

where V_0 is the initial signal. By differentiating both members,

$$\frac{dV}{dt} \propto \frac{d[\mathrm{PdH}]}{dt}. \tag{5}$$

From equations (2)), and (5), we get

$$\frac{dV}{dt} = \frac{aK\sqrt{C}}{1 + K\sqrt{C}}. \tag{6}$$

The fitting curves of equation (6) are presented in figure 4, parameter K has a common value of 0.0080 for each curve, $\boldsymbol{a} = 0.0011$ in the solid curve representing the first hydrogen injection, and $\boldsymbol{a} = 0.00091$ in the dashed curve representing second and third hydrogen injections. The relation between the hydrogen concentrations and local maximum peak heights of the differentiations of signals is explained using the kinetic model of hydrogen absorption to Pd bulk via Langmuir dissociative adsorption on the Pd surface.

4. Conclusion

We performed hydrogen sensing by using the MSS with a 20-nm Pd film. The absorption kinetics could be elucidated by the two-step reaction kinetics of hydrogen absorption into bulk Pd via Langmuir dissociative adsorption on the surface. It was possible to analyze the concentration of hydrogen quantitatively from 25 to 40000 ppm. The merit of using the differentiations to determine hydrogen concentration is the rapid detection, which does not require waiting for signal saturation. The hydrogen MSS sensor could be improved using low hysteresis materials instead of Pd. As MSS is a precise stress sensor, it will be useful for development of hydrogen materials. Moreover, MSS is a good tool to study kinetics on a surface or bulk.

Acknowledgments

We are grateful to C. Nishimura for scientific discussions and A. Ohi, T. Ohki, and N. Ikeda for technical supports in National Institute for Materials Science. This work supported by MEXT/JPSJ KAKENHI Grant Number JP 18H03849 and JST-Mirai Program Grant Number JPMJMI18A3.

ORCID iDs

Taro Yakabe https://orcid.org/0000-0002-2244-5890

References

[1] Hubert T, Boon-Brett L, Black G and Banach U 2011 Hydrogen sensors—A review *Sensors and Actuators B-Chemical* **157** 329–52
[2] Binnig G, Quate C F and Gerber C 1986 Atomic force microscope *Phys. Rev. Lett.* **56** 930
[3] Gimzewski J K, Gerber C, Meyer E and Schlittler R R 1994 Observation of a chemical-reaction using a micromechanical sensor *Chem. Phys. Lett.* **217** 589
[4] Lang H P *et al* 1998 A chemical sensor based on a micromechanical cantilever array for the identification of gases and vapors *Applied Physics a-Materials Science & Processing* **66** S61–4
[5] Okuyama S, Mitobe Y, Okuyama K and Matsushita K 2000 Hydrogen gas sensing using a Pd-coated cantilever *Japanese Journal of Applied Physics Part 1-Regular Papers Short Notes & Review Papers* **39** 3584–90
[6] Chou Y I, Chiang H C and Wang C C 2008 Study on Pd functionalization of microcantilever for hydrogen detection promotion *Sensors and Actuators B-Chemical* **129** 72–8
[7] Manchester F D, San-Martin A and Pitre J M 1994 The H-Pd (hydrogen-palladium) SystemJ. M. *J. Phase Equilibria* **15** 62
[8] Yoshikawa G, Akiyama T, Gautsch S, Vettiger P and Rohrer H 2011 Nanomechanical membrane-type surface stress sensor *Nano Lett.* **11** 1044–8
[9] Yoshikawa G, Akiyama T, Loizeau F, Shiba K, Gautsch S, Nakayama T, Vettiger P, de Rooij N F and Aono M 2012 Two dimensional array of piezoresistive nanomechanical membrane-type surface stress sensor(MSS) with improved sensitivity *Sensors* **12** 15873–87
[10] Imamura G, Shiba K and Yoshikawa G 2016 Smell identification of spices using nanomechanical membrane-type surface stress sensors *Japan. J. Appl. Phys.* **55** 1102B3
[11] Imamura G, Shiba K and Yoshikawa G 2016 Finite element analysis on nanomechanical detection of small particles : toward virus detection *Frontiers in Microbiology* **7** 488
[12] Imamura G, Shiba K, Yoshikawa G and Washio T 2018 Analysis of nanomechanical sensing signals; physical parameter estimation for gas identification *AIP Adv.* **8** 075007
[13] Wang D, Flanagan T B and Kuji T 2002 Hysteresis scans for Pd-H and Pd-alloy-H systems *Phys. Chem. Chem. Phys.* **4** 4244–54
[14] Kay B D, Peden C H F and Goodman D W 1986 Kinetics of hydrogen absorption by PD(110) *Physical Review B* **34** 817–21
[15] Faye O and Szpunar J A 2018 An efficient way to suppress the competition between adsorption of h_2 and desorption of nH_2–Nb complex from graphene sheet: a promising approach to H_2 storage *J. Phys. Chem. C* **122** 28506–17
[16] Faye O, Szpunar J A, Szpunar B and Beye A C 2017 Hydrogen adsorption and storage on Palladium—functionalized graphene with NH-dopant: a first principles calculation *Appl. Surf. Sci.* **392** 362–74

[17] Masel R I 1996 *Principles of Adsorption and Reaction on Solid Surfaces* (Wiley Interscience) p. 244